

RESEARCH ARTICLE

Planar Antenna Arrays Beamforming Using Various Optimization Algorithms

NANCY GHATTAS^{ID}, ATEF M. GHUNIEM, ABDELAZEEM A. ABDELSALAM^{ID}, (Member, IEEE), AND AHMED MAGDY^{ID}, (Member, IEEE)

Electrical Engineering Department, Suez Canal University, Ismailia 41522, Egypt

Corresponding author: Nancy Ghattas (nancyghattas@hotmail.com)

ABSTRACT Due to the importance of beamforming in improving the communication systems performance, this paper presents a novel study of beamforming of planar antenna arrays (PAAs) utilizing the Improved Grey Wolf Optimization (I-GWO) algorithm with the goal of minimizing the peak sidelobe level (PSLL). It is very important to suppress the sidelobe level (SLL) because it minimizes interference and received noise. A two-dimensional (2D) optimization method is presented to find the optimal amplitude excitations and element placements in PAA. The effectiveness of beamforming optimization using the I-GWO is illustrated by comparing it with different metaheuristic algorithms such as Particle Swarm Optimization (PSO), Gravitational Search Algorithm (GSA), Hybrid Particle Swarm Optimization with Gravitational Search Algorithm (PSOGSA), Runge Kutta Optimizer (RUN), Slime Mould Algorithm (SMA), Harris Hawks Optimization (HHO), as well as the original Grey Wolf Optimizer (GWO). Simulation findings show that antenna array beamforming using I-GWO is effective using the 2D optimization method compared to the other algorithms, where the 2D technique achieved the most decreased SLL with the fewest array elements, which helps reduce the cost of the entire system. This clearly shows that I-GWO is very efficient and can be applied to solve different beamforming optimization problems. It can also be used for the radiation pattern synthesis of other antenna array geometries for different wireless networks applications.

INDEX TERMS Beamforming, grey wolf optimizer, optimization algorithms, planar antenna arrays, sidelobe level minimization, smart antennas.

I. INTRODUCTION

The realization of future 6G systems is continually evolving, necessitating systems with superior directivity, low side lobe level (SLL), and narrow beamwidth. In wireless communication systems, smart antennas are regarded as a potential technology. It offers strong solutions for wireless networks that can improve service quality, coverage, and capacity while also enhancing control power [1], [2]. One of the most significant and famous aspects of the advancement of smart antenna technology is adaptive beamforming (ABF) and the massive multi-input-multi-output (MIMO) techniques that are introduced to enhance the capacity of the system. Those techniques are based on using different antenna array geometries according to the required application. The goal

of these techniques is to control different radiation pattern characteristics, for example, SLL suppression and null control [3], [4], [5], [6], [7]. The linear antenna array (LAA) and circular antenna array (CAA) can be regarded as the most frequently utilized types of antenna arrays among the various shapes employed in practical systems. Many research studies are introduced for beamforming optimization for LAA and CAA using different techniques by optimizing one or more array parameters such as element excitation and/or element positions [8], [9], [10], [11], [12], [13], [14], [15], [16], [17], [18], [19], [20], [21], [22], [23]. LAA is the simplest form of antenna array, and CAA can direct the beam pattern in any desired direction. However, practically, CAA is more complex than LAA. Improving the beam directivity of an antenna can enhance the energy efficiency of a communication system; this requires more directive antennas. Planar Antenna Arrays (PAA) present an intriguing area for

The associate editor coordinating the review of this manuscript and approving it for publication was Kai Lu^{ID}.

research, where planar arrays are mainly used to get more directive and symmetric patterns. Its major application areas include remote sensing, search and tracking radars, satellite communications, etc. Many studies introduce PAA optimization by controlling single parameters, for example, element excitations or spacing between elements [24], [25], [26], [27], [28], [29], [30], [31], [32], [33], [34], [35]. In this paper, PAA beamforming optimization is introduced by optimizing both amplitude excitations and element positions using two dimensional (2D) optimization. To the authors' knowledge, the 2D method has not been applied before to PAA. Selecting an optimal set of parameters to achieve the expected beam pattern is called antenna array beamforming. The beam pattern optimizations of antenna arrays, however, become extremely challenging non-linear problems since the relations between these parameters are not easy. Therefore, it is crucial to understand how to improve antenna array beam patterns and decrease maximum SLL. There are several conventional and classical antenna array SLL suppression methods, such as the Taylor synthesis method [36], the Chebyshev synthesis method [37], and the convex optimization method [38]. However, the increasing requirements in communication systems imply more focus on the implementation of beamforming optimizations using the recent optimization algorithms in smart antennas. Swarm intelligence optimization algorithms, however, provide advantages over conventional antenna array synthesis methods in specific applications that are based on antenna array systems, making them more appropriate for these applications. The conventional Chebyshev synthesis approach, for example, has a number of limitations when used with large antenna arrays. Additionally, this approach has a high time cost. By applying the convex optimization method to the antenna array beam pattern synthesis problem, it is also necessary to remove some restrictions. As a result, real applications cannot use it. Without taking into account the limitations of the optimization problem, swarm intelligence optimization methods can be applied to nearly any application. Since these techniques can be viewed as practical approaches, where the swarm intelligence optimization as well as the evolutionary computation algorithms are common methods for the SLL suppressions of the antenna arrays [39], these methods can be regarded as practical approaches, and thus we will consider using them as the optimizer in this paper as they have become the focus of more and more researchers. A wide variety of algorithms have been introduced and their effectiveness to solve different optimization problems has been demonstrated, such as the application of Harris Hawks Optimization (HHO) to solve real-world optimization problems such as manufacturing optimization problems, pattern recognition problems, power quality problems, and drug design problems [40], [41], [42]. The introduction of the Slime Mould Algorithm (SMA) in [43] and its application in various fields to solve optimization challenges, including scheduling optimization, machine learning optimization, and image segmentation [44]. Also, Particle Swarm Optimization (PSO) is a very well-established and powerful

population-based metaheuristic that has been applied to solve several optimization problems [45], [46], [47], [48]. Also, Runge Kutta Optimizer (RUN) and its application in different fields are presented in [49] and [50]. Also, the introduction of algorithm hybridization to strengthen its effectiveness, for example, Hybrid Particle Swarm Optimization with Gravitational Search Algorithm (PSOGSA) are applied in [51] and [52].

Among the various global optimization techniques, the Grey Wolf Optimizer (GWO) has been attracting considerable attention since its introduction in 2014 by Heidari et al. [53], [54]. It has been used to solve optimization problems in many fields, such as medical, bioinformatics, computer science, and engineering.

However, it may experience a lack of population and an imbalance between exploitation and exploration, which may not be enough to find the optimal solution. Many improvements are introduced to enhance the GWO algorithm for global optimization problems [55], [56], [57], [58]. Recently, an enhanced algorithm named Improved Grey Wolf Optimizer (I-GWO) has been introduced [59] to overcome GWO deficiencies. In I-GWO, utilizing a new search strategy named dimension learning-based hunting (DLH) [60]. I-GWO has been evaluated and benchmarked to explain its superiority over other algorithms in [59].

The purpose of this paper is to study the design and beamforming optimization of PAA using the I-GWO optimization algorithm with the goal of suppressing the peak (PSLL), which is a key problem in antenna array synthesis in 5G communication systems. To achieve this goal, optimization algorithms are used to find the optimum amplitude and position of array elements using 2D optimization. To the authors' knowledge, this is the first time to apply the 2D optimization method for PAA using the optimization algorithms. The effectiveness of using I-GWO in achieving the design goals is illustrated by comparing it with other existing algorithms like PSO, GSA, PSOGSA, RUN, SMA, HHO, and GWO. I-GWO has achieved the most minimized SLL with the minimum number of array elements compared to other algorithms.

A. PAPER CONTRIBUTIONS

The following is an overview of this paper's contributions:

- The optimization problem fitness function is formulated for radiation pattern synthesis and the SLL suppression for PAA for wireless communications.
- To overcome the drawbacks of conventional GWO, the I-GWO algorithm is used to solve the formulated SLL suppression optimization problems.
- Simulation is conducted to further verify the effectiveness and performance of the proposed I-GWO algorithm for the SLL reductions of PAAs in comparison with other algorithms. Simulation is performed first by single parameter optimization. Second, the 2D optimization method is applied to PAA to verify

the effectiveness of these methods in radiation pattern synthesis.

- Additionally, electromagnetic (EM) simulations using FEKO software are run to evaluate the effectiveness of various strategies in an EM environment.

B. ROADMAP

The rest of this paper is organized as follows: Section II presents the related work for research in antenna array pattern synthesis using optimization algorithms for different array geometries. Section III presents the PAA geometry, array factor, and fitness function. In Section IV, the I-GWO algorithm is explained in detail alongside other algorithms like PSOGSA and GWO. In Section V, simulation results using single parameter optimization and 2D optimization using I-GWO in comparison to various techniques are presented. Concluding remarks and future work are provided in Sections VI and VII, respectively.

II. LITERATURE REVIEW

Many studies have introduced the antenna array beam pattern synthesis with different geometries using evolutionary algorithms with the goal of suppressing the SLL. For example, the synthesis of non-uniform LAA is introduced using the Genetic Algorithm (GA) by null control and SLL suppression [8], [9]. In [10] and [11] the authors optimize the different antenna array parameters for minimizing the SLL using the Cuckoo Search (CS) algorithm for LAA and CAA. The PSO algorithm is introduced for beamsteering applications to minimize the SLL and null control in [12], [13], [14]. Gravitational Search Algorithm (GSA) is applied for the design and optimization of dipole LAA in [15], and also for adaptive beamforming applications in [16]. Improved biogeography-based optimization [IBBO] is used to suppress the maximum SLL for LAA and CAA [17]. Uniform and sparse linear antenna arrays pattern synthesis using the Mayfly (MF) Algorithm is presented in [18]. Broadband design of whip antenna Using the Grasshopper Optimization Algorithm (GOA) is introduced in [19]. Reference [20] introduce a novel Sparrow Search Algorithm (SSA) for LAA SLL reduction. GWO algorithm is applied to antenna array pattern synthesis [21], [22]. Optimization of CAA using a Differential Search Algorithm (DSA) is applied in [23]. However, it is challenging to adjust SLL and primary in a planar array, where the major application of planar arrays is to obtain more symmetric and directed patterns. Satellite communications, search and tracking radars, and remote sensing are a few of its main application areas [24], [25], [26]. Different planar antenna array patterns are synthesized using Biogeography Based Optimization (BBO) [27]. SLL suppression of antenna arrays using an Improved Chicken Swarm Optimization (ICSO) in [28]. The application of Concentric Circular antenna array (CCA) pattern synthesis using Moth Flame Optimization (MFO) in [29]. Sparse thinned planar array using Teaching Learning-Based Optimization (TLBO) is presented in [32]. Planar thinned array synthesis

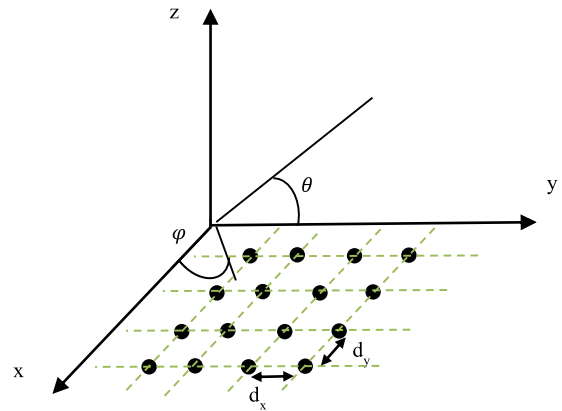


FIGURE 1. Planar antenna array (PAA) with $M \times N$ elements for spacing dx and dy .

using modified Brain Storm Optimization (BSO) is described in [33]. Wind Driven Optimization (WDO) is used in [34] to minimize the SLL by controlling amplitude and phase excitations. Optimization for uniform planar antenna arrays to minimize the SLL using GA is studied in [35].

III. ARRAY FACTOR AND FITNESS FUNCTION

The antenna array factor is affected by the geometry of the antenna arrays (linear, rectangular, circular, etc.), the spacing between the elements, and the amplitudes and phases of the excitation of the elements.

The model and array factor of PAA that used beamforming optimization are shown in this section.

A. ARRAY FACTOR FOR PAA

First, assume LAA, where Melements are positioned along the x-axis with symmetric excitations. The following can be used to represent the array factor for symmetric LAA [61]:

$$AF_{LAA}(\theta, \varphi) = 2 \sum_{m=1}^M A_x e^{j(m-1)(kd_x \sin \theta \cos \varphi + \beta_x)}, \quad (1)$$

where M is the number of elements on the x-axis; A_x is the m-th element amplitude excitation; β_x is the m-th element phase excitation; d_x is the m-th element position, θ is the elevation angle; and φ is the azimuth angle. k is the wave number where $k = \frac{2\pi}{\lambda}$; and λ is the wavelength.

Second, if N of such linear arrays are placed next to each other in the y direction, a rectangular array will be formed as shown in Fig. 1. If one considers the case of uniform unitary excitation, the entire array factor can be written as:

$$AF_{PAA}(\theta, \varphi) = A_{xy} \sum_{m=1}^M e^{j(m-1)(kd_x \sin \theta \cos \varphi + \beta_x)} \times \sum_{n=1}^N e^{j(n-1)(kd_y \sin \theta \sin \varphi + \beta_y)} \quad (2)$$

$$A_{xy} = A_x A_y \quad (3)$$

The optimization problem is to determine the amplitude excitation and the positions of the elements on the x-y plane that yield a radiation pattern with minimum SLL at specific

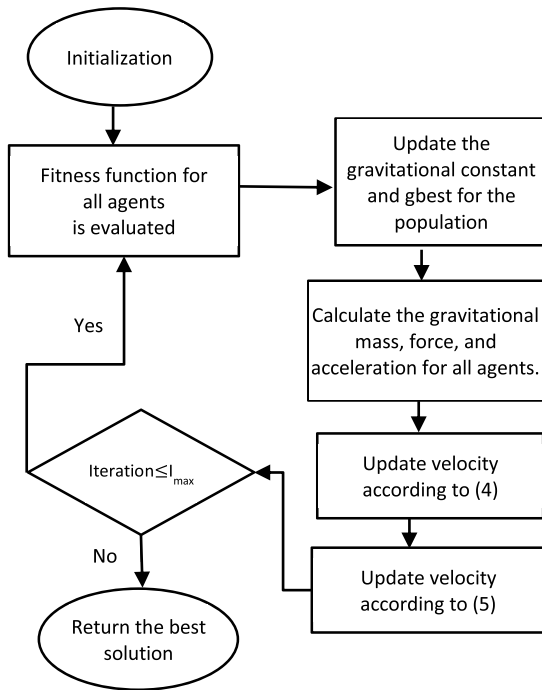


FIGURE 2. Flow chart for PSO-GSA.

directions. Using the optimization algorithm, we will determine the parameters of the AF.

B. THE FITNESS FUNCTION

Many factors can be used to evaluate the fitness function, such as directivity, gain, SLL, size, and weight, depending on the application. For the current problem, we are interested in designing the geometry for a planar antenna with a minimum average SLL. Interference suppression and SLL reduction can be obtained by controlling array factor parameters. To achieve this goal, the following function is used to evaluate the normalized fitness function:

$$\text{Fitnessfunction} = \min(\max\{20 \log |AF_{PAA}(\theta, \varphi)|\}), \quad (4)$$

IV. OPTIMIZATION TECHNIQUES

The GWO and I-GWO algorithms will be described in detail in this section, along with the PSO-GSA method, which will be used for PAA radiation pattern optimization.

A. HYBRID PARTICLE SWARM OPTIMIZATION AND GRAVITATIONAL SEARCH ALGORITHM (PSO-GSA)

PSO-GSA is a hybrid population-based algorithm that is a combination of (PSO) and (GSA). Merging the optimization algorithms is a way to balance the overall exploration and exploitation abilities. where it is presented by Mirjalili in [51]. PSO is one of the most widely used evolutionary algorithms in hybrid methods due to its simplicity, convergence speed, and ability to search for a global optimum. combine the functionality of both algorithms. PSO-GSA adds the exploitation capability of PSO with the exploration feature of GSA

in one hybrid algorithm. PSO-GSA has been applied to a circular antenna array for beamforming optimization, which demonstrates capability in antenna pattern synthesis [52]. The concept of the PSO-GSA algorithm is to integrate GSA’s local search with PSO’s social thinking (gbest). As shown in (5), the combination of these algorithms is as follows [51]:

$$V_i(t + 1) = w \times V_i(t) + c'_1 \times \text{rand} \times a_{xi}(t) + c'_2 \times \text{rand} \times (\text{gbest} - X_i(t)), \quad (5)$$

where $V_i(t)$ is the velocity of the agent i at iteration t , c'_1 and c'_2 are weighting factors, w is a weighting function, rand is a random number between 0 and 1, $a_{xi}(t)$ represents the acceleration of agent i at each iteration t , and gbest is the best solution; the positions are updated as follows in each iteration:

$$X_i(t + 1) = X_i(t) + V_i(t + 1). \quad (6)$$

Fig. 2 depicts the PSO-GSA process steps. All agents are initialized at random. Each agent is taken into account as a candidate solution. The gravitational force, gravitational constant, and resulting force between agents are determined after initialization. The best solution up to that point should be updated in every iteration. All agents’ velocities can be estimated using (5). Finally, the positions of agents are defined using (6). If an end criterion is satisfied, the updating of velocities and locations will terminate.

B. GREY WOLF OPTIMIZER (GWO)

GWO was presented by Heidari et al. in [53] in 2014. It has been applied to solve different optimization problems in many fields, such as engineering, machine learning, medical, and bioinformatics as presented in [54]. The GWO algorithm is also applied to LAA for optimal pattern synthesis [21], [22]. GWO is a metaheuristic nature inspired algorithm that mimics the hunting mechanism of grey wolf groups. It considers four levels of wolves in a hierarchy way, as α in the top level dominates all the wolves and its position represents the best solution. The β and δ wolves positions represent the second and third best solutions, respectively. The fourth level is named (ω) wolve. Theoretically, hunting activity is modeled in three phases: encircling, hunting, and attacking the prey. GWO’s flowchart is described in Fig. 3. First, initialization for all agents is done within the search space. The fitness function is calculated for all agents represented by the wolves’ positions. Then, GWO’s best position is calculated. And it is updated in every iteration. Finally, by repeating these steps, the α ’s position that represents the best location can be found. In GWO, the candidate solution is represented by the position of grey wolves, while the best solution is represented by the position of prey in each iteration. Mathematically, the hunting mechanism assumes that the top three levels have a good knowledge of the prey position and that the (ω) wolves update their location based on the three top level wolves. The three best solutions considered by α , β , and δ wolves’ location of the prey. This pushes the other wolves denoted by

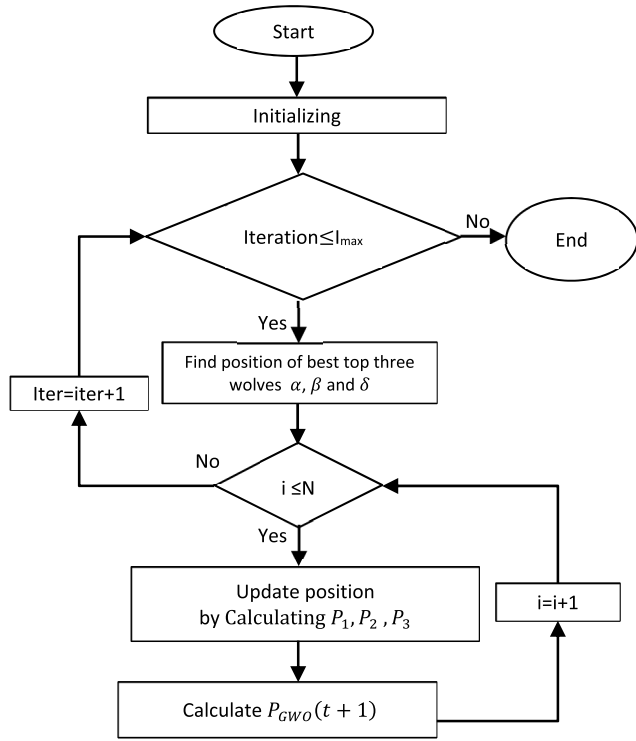


FIGURE 3. Flow chart for GWO.

(ω) to follow them. Hunting behavior can be represented as follows:

$$\begin{aligned} U_\alpha &= |V_1 \times P_\alpha(t) - P(t)|, \\ U_\beta &= |V_2 \times P_\beta(t) - P(t)|, \\ U_\delta &= |V_3 \times P_\delta(t) - P(t)|, \end{aligned} \quad (7)$$

$$\begin{aligned} P_1(t) &= P_\alpha(t) - W_1 \times U_\alpha(t), \\ P_2(t) &= P_\beta(t) - W_2 \times U_\beta(t), \\ P_3(t) &= P_\delta(t) - W_3 \times U_\delta(t), \end{aligned} \quad (8)$$

where $P(t)$ indicates the position vector of a grey wolf, t is the current iteration. V and W are the coefficient vectors calculated by Eqs. (9) and (10). P_α , P_β , and P_δ represent the first three best solutions at iteration t .

$$V = 2 \times s_2, \quad (9)$$

$$W = 2 \times r \times s_1 - r(t), \quad (10)$$

s_1 , s_2 represent constant numbers in the interval (0, 1) and they are updated at each iteration randomly, and the elements of the vector r are linearly decreased from 2 to 0 over the course of iterations using equation (11).

$$r(t) = 2 - \frac{2 \times t}{I_{max}}, \quad (11)$$

$$P_{i-GWO}(t+1) = \frac{P_1(t) + P_2(t) + P_3(t)}{3}, \quad (12)$$

where $P_{i-GWO}(t+1)$ represents the position of the grey wolf in next iteration.

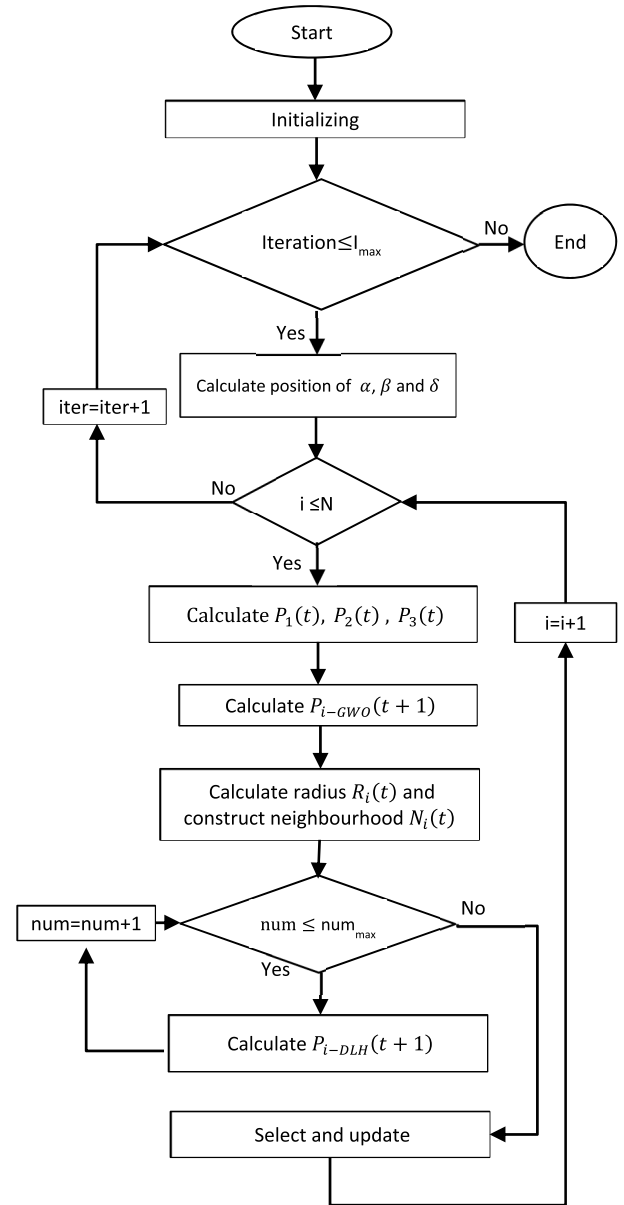


FIGURE 4. Flow chart for I-GWO [59].

C. IMPROVED GREY WOLF OPTIMIZER (I-GWO)

Although GWO is simple to implement and very efficient, there is an imbalance between exploitation and exploration, which causes the population to lose diversity too early because the positions of wolves are updated based on the top-level wolves' locations. A number of improvements to the basic GWO algorithm have been introduced to overcome GWO's deficiencies, and provide better performance to avoid the local optima and accelerate convergence speed.

Examples of improved GWO algorithms; weighted distance Grey Wolf Optimizer (wdGWO) algorithm, where a weighted average of the best answers rather than a simple arithmetic average is calculated [55]. Also, a hybrid Grey Wolf Optimizer–Sine Cosine Algorithm (HGWOCSA) is proposed in [56] which benefits from the hybridization of

GWO and SCA. Alomoush et al. proposed a hybrid harmony search and GWO named GWO-HS with an opposition learning strategy to solve global optimization problems [57]. In these improved algorithms, the global convergence and exploitation ability for unimodal problems improved, but the exploration for multimodal functions and the balance for composition functions remained insufficient. Recently, I-GWO was introduced by Heidari et al. to improve GWO deficiencies, and its performance is evaluated on the CEC 2018 benchmark suite, where it is used to solve four engineering problems, including the pressure vessel design, the welded beam design, and the optimal power flow problems in [59]. The results of the proposed algorithm on engineering design problems demonstrate its efficiency and applicability.

Besides the best solution in (12) from the conventional GWO, the I-GWO proposed another candidate's updated position based on the DLH strategy in [60]; this new search strategy is inspired by the individual hunting behavior of grey wolves. This new search strategy improves the transition between local and global solutions and resolves the lack of population diversity.

The DLH search strategy can work as follows: the position of the i -th wolf in the t -th iteration $P_i(t)$ is created where an individual wolf is learned by its neighbors. DLH search strategy generates another candidate for the new position of wolf $P_i(t)$ named $P_{i-DLH}(t+1)$. First, a radius $R_i(t)$ is calculated using the Euclidean distance between the current position of $P_i(t)$ and $P_{i-GWO}(t+1)$ which is given by,

$$R_i(t) = \|P_i(t) - P_{i-GWO}(t+1)\|. \quad (13)$$

Then, the neighbors of $P_i(t)$ denoted by $N_i(t)$ are constructed in (14) with respect to radius $R_i(t)$, where D_i is Euclidean distance between $P_i(t)$ and $P_j(t)$.

$$N_i(t) = \{P_j(t) \mid D_i(P_i(t), P_j(t)) \leq R_i(t), P_j(t) \in Pop\}. \quad (14)$$

where Pop is the matrix to store the whole population of wolves. Once the neighborhood of $P_i(t)$ is constructed, multiple neighbor learning is performed, where the d -th dimension of the superior candidate is selected by comparing the fitness values of the two candidates $P_{i-GWO}(t+1)$ and $P_{i-DLH}(t+1)$.

$$P_{i-DLH}(t+1) = P_{i,d}(t) + \text{rand} \times (P_{n,d}(t) - P_{r,d}(t)), \quad (15)$$

$$P_i(t+1) = \begin{cases} P_{i-GWO}(t+1), & \text{if } F(P_{i-GWO}) < f(P_{i-DLH}) \\ P_{i-DLH}(t+1) & \text{otherwise,} \end{cases} \quad (16)$$

I-GWO flowchart is illustrated in Fig. 4. After the initialization phase, the fitness function evaluates the wolves' positions. Then, the DLH position is calculated. The best solution is selected by comparing GWO and DLH best results

TABLE 1. Parameters settings of the employed algorithms.

Algorithm	Settings
I-GWO [59]	r decreased from 2 to 0, $s_1, s_2 = [0,1]$
GWO [53]	r decreased from 2 to 0, $s_1, s_2 = [0,1]$
PSOGSA [51]	$c'_1=0.5$ and $c'_2=1.5$, $\omega = [0,1]$
GSA [15]	$G_0 = 100, \alpha = 20$
RUN [49]	$a = 20, b = 12$
SMA [43]	$r [0,1]$
PSO [13]	$c_1=c_2=2, \omega = 0.4 - 0.9, r_1, r_2 = [0,1]$

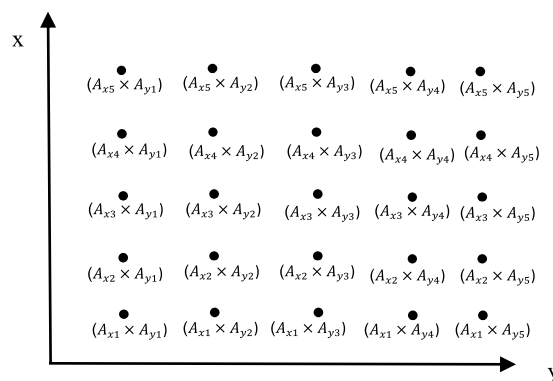


FIGURE 5. Elements amplitude distribution for PAA in x-y coordinates.

in every iteration. In order to update the new position, if the fitness value of the selected candidate is less than $P_i(t)$, $P_i(t)$ is updated by the selected candidate. Otherwise, $P_i(t)$ remains unchanged. Finally, after performing this procedure for all individuals, the counter of iterations is increased by one, and search can be iterated until the predefined number of iterations is reached.

V. SIMULATION RESULTS

In this section, the IGWO algorithm for optimizing PAAs is evaluated. The proposed scheme is installed on an Intel®Core™i-8550U CPU @ 1.80 GHz 1.99 GHz with a setup memory of 6.00 GB and a 64-bit operating system. The PAA array pattern optimization is applied using I-GWO by single parameter optimization (amplitude excitation only A_{mn} and element position only d_x and d_y), and then by applying 2D optimization by optimizing both amplitude excitation and elements positions for the goal of SLL minimization. Simulation results are compared with other existing optimization algorithms to show the effectiveness of I-GWO techniques; PSO, GSA, PSOGSA, GWO, SMA, RUN, and HHO. Table 1 contains a list of the comparative techniques' parameter settings. The parameters used were those employed by the original author of the study or those often employed by other studies. In [59], the control parameter r in GWO and I-GWO is set to decrease linearly

TABLE 2. FNBW and PSLL results for the 5 × 5 element PAA using amplitude only optimization.

Method	Amplitude excitation ($A_{x1}, A_{x2}, \dots, A_{x5}$) / ($A_{y1}, A_{y2}, \dots, A_{y5}$)	PSLL (dB)	FNBW
I-GWO	(0.8297, 0.8493, 0.9659, 0.8599, 0.8010) / (0.2715, 0.8510, 0.3294, 0.6659, 0.9433)	-13.74	50°
GWO	(0.8439, 0.8935, 0.9989, 0.8771, 0.8432) / (0.6233, 0.3064, 0.7154, 0.3210, 0.0328)	-13.7	50°
PSOGSA	(0.8521, 0.8614, 0.9916, 0.8916, 0.8211) / (0.7910, 1.0000, 0.3359, 0.2760, 0.4907)	-13.69	50°
GSA	(0.7597, 0.8378, 0.9312, 0.8077, 0.8110) / (0.5100, 0.3690, 0.4394, 0.4489, 0.7612)	-13.7	50°
RUN	(0.6959, 0.7439, 0.8469, 0.7540, 0.7346) / (0.2305, 0.0663, 0.6392, 0.0701, 0.1538)	-13.7	50°
SMA	(0.8461, 1.0000, 1.0000, 0.8215, 0.8389) / (1.0000, 0.0556, 0.3007, 0.5237, 0.3310)	-12.56	50°
HHO	(0.2579, 0.3400, 0.3720, 0.3089, 0.3663) / (0.2808, 0.2999, 0.3833, 0.3478, 0.3639)	-13.51	50°
PSO	(0.5359, 0.6049, 0.6640, 0.5670, 0.5827) / (0.0214, 0.9923, 0.7524, 0.1294, 0.9497)	-13.69	50°

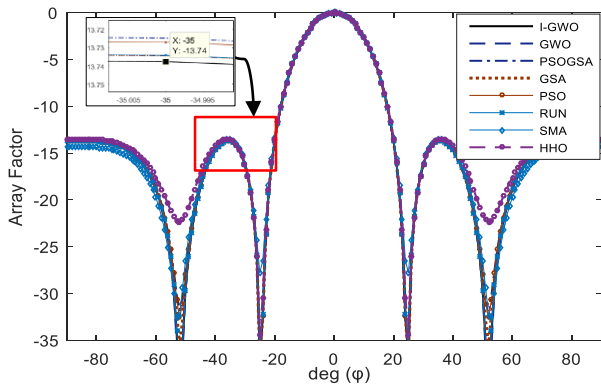


FIGURE 6. Normalized array factors of the 5 × 5 element PAA (Amplitude-only optimization).

from 2 to 0 and the constants s_1, s_2 are in the range of [0,1]. In SMA [43], r is a random value in the range [0,1]. In PSOGSA [51], c_1' and c_2' are the individual learning factor and Social learning factor, ω is the weighting function. In PSO [13], c_1 and c_2 are the learning factors, ω is the inertial weight. In GSA, Gravitational constant G_0 is 100 and Gradient constant α is 20 same as used in [15], and RUN algorithm constants, a and B , are 20 and 12 respectively, from [49].

The efficiency of the IGWO algorithm for the PAAs pattern synthesis is confirmed by EM simulations using FEKO software. The number of iterations is 400, and the search agent is 30 and number of run is 25, where the average result is presented in this paper. Based on the no free lunch theorem (NFLT) [62], there is no optimization technique that can perfectly operate in all problems. However, it was found, from

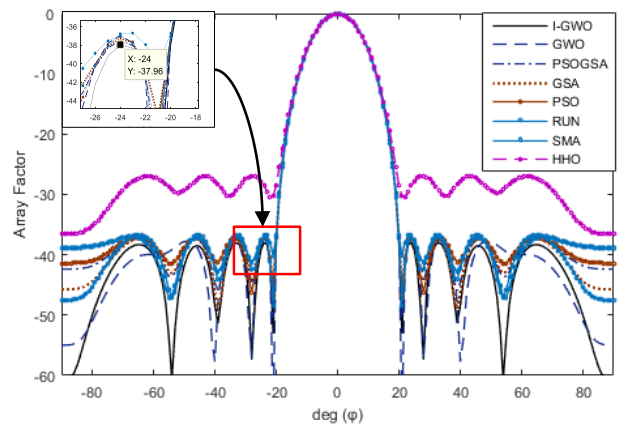


FIGURE 7. Normalized array factors of the 10 × 10 element PAA (Amplitude-only optimization).

this study and simulation results, that the I-GWO algorithm is quite perfect in solving the antenna array beamforming problems.

A. PAA AMPLITUDE EXCITATION OPTIMIZATION

This section presents PAA beamforming optimization for optimum minimization of PSLL through the control of amplitude excitations (A_x and A_y) while assuming uniform phase excitation ($\beta_x = \beta_y = 0$) with fixed spacing between elements ($\lambda/2$) using the normalized fitness function in (4). The array factor will be applied as follows:

$$AF_{PAA}(\theta, \varphi) = A_{xy} \sum_{m=1}^M e^{j((m-0.5)\pi \sin\theta \cos\varphi)} \sum_{n=1}^N e^{j((n-0.5)\pi \sin\theta \sin\varphi)} \quad (17)$$

TABLE 3. FNBW and PSLL results for the 10 × 10 element PAA using amplitude only optimization.

Method	Amplitude excitation ($A_{x1}, A_{x2}, \dots, A_{x10}$)/ ($A_{y1}, A_{y2}, \dots, A_{y10}$)	PSLL (dB)	FNBW
I-GWO	(0.1557, 0.3415, 0.6022, 0.8390, 0.9728, 0.9588, 0.7946, 0.5457, 0.3011, 0.1134) / (0.6657, 0.9315, 0.9716, 0.6446, 0.6690, 0.2666, 0.2843, 0.4744, 0.8085, 0.5350)	-37.96	42°
GWO	(0.1494, 0.3442, 0.5956, 0.8457, 0.9632, 0.9642, 0.7801, 0.5409, 0.2952, 0.0985) / (0.0308, 0.0030, 0.4711, 0.0048, 0.0484, 0.6339, 0.7361, 0.1396, 0.9774, 0.6611)	-36.99	42°
PSOGSA	(0.1861, 0.3881, 0.6566, 0.8846, 1.0000, 0.9570, 0.7717, 0.5121, 0.2703, 0.0994) / (0.5238, 0.4942, 0.6641, 0.6584, 0.8686, 0.9718, 0.0634, 0.0014, 0.2621, 0.9574)	-37.48	42°
GSA	(0.0947, 0.2472, 0.4670, 0.7038, 0.8797, 0.9162, 0.8176, 0.6101, 0.3625, 0.1716) / (0.2685, 0.2502, 0.3644, 0.3326, 0.3386, 0.5444, 0.2636, 0.5541, 0.3030, 0.4002)	-37.31	42°
RUN	(0.1940, 0.4110, 0.6744, 0.8960, 0.9965, 0.9393, 0.7519, 0.5013, 0.2637, 0.1087) / (0.6684, 0.2532, 0.5079, 0.1688, 0.2938, 0.5184, 0.4778, 0.1510, 0.0832, 0.3413)	-36.82	42°
SMA	(0.0602, 0.1653, 0.3183, 0.4924, 0.6116, 0.6531, 0.5790, 0.4373, 0.2640, 0.1275) / (0.7843, 0.0881, 0.7411, 0.0000, 0.3263, 0.0287, 1.0000, 0.1019, 0.0083, 0.1892)	-36.99	42°
HHO	(0.1113, 0.1113, 0.3065, 0.5496, 0.5962, 0.6265, 0.5120, 0.4020, 0.2217, 0.1113) / (0.2593, 0.1113, 0.4795, 0.1113, 0.5046, 0.5814, 0.6138, 0.1113, 0.1113, 0.4700)	-26.93	42°
PSO	(0.1227, 0.2889, 0.5561, 0.8094, 1.0063, 1.0414, 0.9228, 0.6735, 0.4067, 0.1749) / (0.7779, 0.1861, 0.8423, 0.2788, 0.7838, 0.7744, 0.4950, 1.4884, 0.1123, 0.2804)	-37.13	42°

The following examples were studied in the SLL region of $\varphi_{SL} = [-80^\circ, -25^\circ]$. The lower and upper limits X_L and X_U are set to 0 and 1, respectively. Simulation results are compared with other optimization algorithms; PSO, GSA, PSOGSA, GWO, SMA, RUN, and HHO.

Example 1 illustrates the SLL suppression for an 5×5 element array. The amplitude excitation distribution for PAA in x-y coordinates is shown in Fig. 5. The comparison results in terms of SLL and first null beamwidth (FNBW) are shown in Table 2, normalized array factor comparison for the PAA is shown in Fig. 6. I-GWO provides SLL of -13.74 dB and FNBW of 50° , while for GWO, GSA and RUN, SLL is -13.7 dB which is higher than I-GWO by 0.04 dB for same FNBW. For PSOGSA and PSO, SLL is equal to -13.69 dB which is greater than I-GWO SLL by 0.05dB. For HHO and SMA, SLL is -13.51 dB and -12.56 dB respectively.

In example 2, the number of elements is set to 10×10 . SLL region is $\varphi_{SL} = [-80^\circ, -21^\circ]$. The comparison results are shown in Table 3, normalized array factor comparison for the PAA is shown in Fig. 7. SLL in the case of I-GWO is -37.96 dB, and FNBW is 42° , while for GWO and SMA, SLL is -36.99 dB which is higher than I-GWO by 0.97 dB for same FNBW. For PSOGSA SLL is equal to -37.48 dB which is greater than I-GWO SLL by 0.48 dB. For the other algorithms SLL are -37.31 dB, -37.13 dB, -36.82 dB and -26.93 dB for GSA, PSO, RUN and HHO respectively.

It can be concluded from examples 1 and 2, I-GWO results in more enhancements compared with other methods. And it can be noted that all algorithms result in SLL minimization

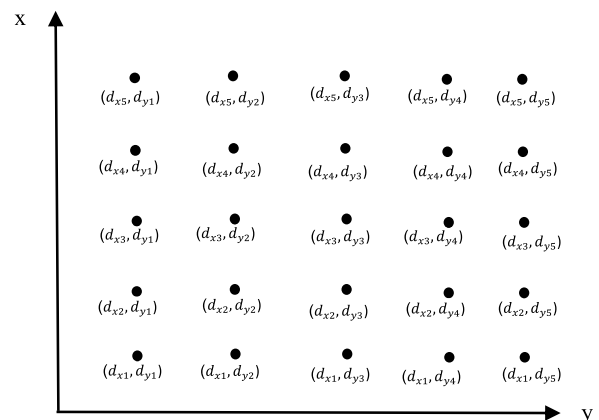


FIGURE 8. Elements position distribution for PAA in x-y coordinates.

when increasing the number of array elements, while FNBW is minimized, that means the tradeoff between SLL and FNBW.

B. PAA POSITION-ONLY OPTIMIZATION

This section presents SLL minimization using array element position optimization (d_x and d_y), while using uniform amplitude ($A_{xy} = 1$) and phase excitations ($\beta_x = \beta_y = 0$), using the normalized fitness function in (4). Now the array factor becomes,

$$\begin{aligned}
 &AFPAA(\theta, \varphi) \\
 &= \sum_{m=1}^M e^{j(m-1)(kd_x \sin\theta \cos\varphi)} \sum_{n=1}^N e^{j(n-1)(kd_y \sin\theta \sin\varphi)} \quad (18)
 \end{aligned}$$

TABLE 4. FNBW and PSLL results for the 5 × 5 element PAA using position only optimization.

Method	Element position ($d_{x1}, d_{x2}, \dots, d_{x5}$) / ($d_{y1}, d_{y2}, \dots, d_{y5}$)	PSLL (dB)	FNBW
I-GWO	(0.5027, 1.2224, 1.8568, 2.3569, 2.9973) / (0.9996, 1.4996, 2.0000, 2.5404, 3.0409)	-15.65	28°
GWO	(0.8033, 1.4431, 1.9431, 2.5776, 3.3008) / (0.9554, 1.4702, 2.2609, 2.8832, 3.4342)	-14.63	28°
PSOGSA	(0.8578, 1.5806, 2.2136, 2.7136, 3.3516) / (0.5022, 1.0078, 1.5323, 2.5318, 3.5083)	-14.28	28°
GSA	(0.6165, 1.3064, 2.1096, 2.8202, 3.6494) / (0.7275, 1.5176, 2.2314, 2.9948, 3.6926)	-12.25	30°
HHO	(0.5537, 1.2376, 1.8547, 2.4085, 3.0584) / (0.8626, 1.8608, 2.8590, 3.5433, 4.0970)	-11.3	28°
SMA	(0.5978, 1.3196, 1.9519, 2.4520, 3.0897) / (0.5124, 1.2716, 1.7718, 2.2718, 3.2713)	-13.5	30°
RUN	(0.5002, 1.1385, 1.6389, 2.2718, 2.9940) / (0.5000, 1.0025, 1.6473, 2.1573, 2.6575)	-13.46	28°
PSO	(0.8034, 1.4871, 2.0733, 2.5760, 3.0822) / (1.3579, 1.8579, 2.4579, 2.9879, 3.6479)	-13.59	28°

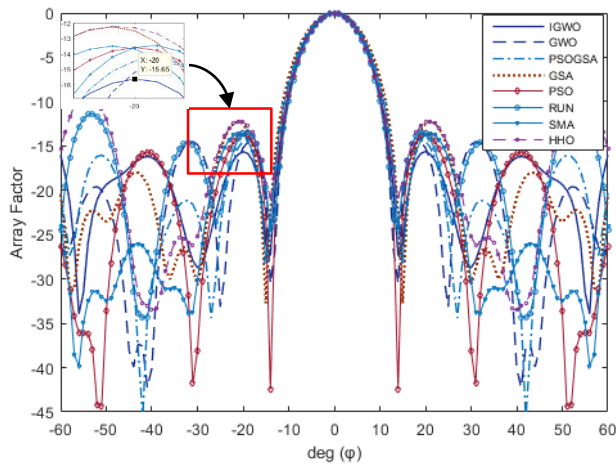


FIGURE 9. Normalized array factors of the 5 × 5 element PAA (position-only optimization).

Two cases were tested for a number of elements 5 × 5 and 10 × 10. The proper placement of antennas in the array is very important because if antennas are placed too close to each other, this leads to mutual coupling effects, and if antennas are placed too far away, this leads to grating lobes. Thus, conditions must be satisfied for antenna position optimization to be lower than 0.5λ. The lower and upper limits X_L and X_U are set to 0.5 and 1, respectively. Example 3 illustrates the design optimization of an 5 × 5 element antenna array. The sidelobe region is $\varphi_{SL} = [-80^\circ -20^\circ]$. Simulation results are compared with other optimization algorithms; PSO, GSA, PSOGSA, GWO, SMA, RUN, and HHO. Elements position distribution for PAA in x-y coordinates is shown in Fig.8.

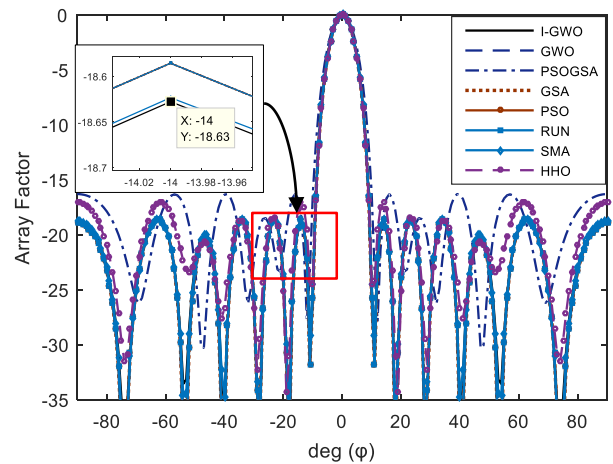


FIGURE 10. Normalized array factors of the 10 × 10 element PAA (position-only optimization).

Normalized array factor for the PAA is shown in Fig. 9. The comparison results are shown in Table 4. which shows that I-GWO provides SLL of -15.65dB and FNBW is 28°, while for GWO, the SLL is -14.63 dB which is higher than I-GWO by 1.02dB for same FNBW. For PGOGSA, RUN, SMA, PSO, HHO and GSA, SLL is -14.28 dB, -13.46 dB, -13.5 dB, 13.59 dB, and -11.3dB respectively. In example 4, the number of elements is set to 10 × 10. SLL region is $\varphi_{SL} = [-80^\circ -11^\circ]$. The comparison results are shown in Table 5, normalized array factor comparison for the PAA is shown in Fig. 10. SLL in the case of I-GWO is -18.63dB, and FNBW is 22°, while for SMA, HHO and PSOGSA, are -18.62 dB, -17.03 dB and

TABLE 5. FNBW and PSLL results for the 10 × 10 element PAA using position only optimization.

Method	Element position ($d_{x1}, d_{x2}, \dots, d_{x10}$) / ($d_{y1}, d_{y2}, \dots, d_{y10}$)	PSLL (dB)	FNBW
I-GWO	(0.9011, 1.6378, 2.3058, 2.8159, 3.3233, 3.8234, 4.3255, 4.8987, 5.5825, 6.3544) / (0.6524, 1.2132, 2.0735, 3.0011, 3.5561, 4.1643, 4.6715, 5.3374, 5.9172, 6.6162)	-18.63	22°
GWO	(0.5106, 1.2608, 1.9289, 2.4806, 2.9806, 3.4806, 3.9950, 4.5282, 5.2093, 5.9630) / (0.8632, 1.7099, 2.3933, 2.9959, 3.5062, 4.3404, 4.9482, 5.7468, 6.3447, 6.9099)	-18.59	22°
PSOGSA	(0.5293, 1.3583, 2.3583, 2.9583, 3.7583, 4.3583, 5.0083, 5.5283, 6.1083, 6.7883) / (0.5145, 1.0145, 1.5245, 2.0745, 2.5945, 3.3945, 4.1745, 5.0545, 5.9345, 6.4945)	-16.7	22°
GSA	(0.3068, 1.0357, 1.6443, 2.1119, 2.6205, 3.0777, 3.5482, 4.0918, 4.7624, 5.5004) / (0.5693, 1.0693, 1.6093, 2.1393, 2.6693, 3.1893, 3.7893, 4.4893, 5.0393, 5.5693)	-18.59	22°
HHO	(0.5001, 1.2706, 2.0475, 2.5476, 3.1232, 3.6233, 4.1234, 4.7002, 5.2397, 5.9420) / (0.5001, 1.0002, 1.8412, 2.6396, 3.4527, 4.2658, 4.8293, 5.6425, 6.4552, 6.9554)	-17.03	20°
SMA	(0.5035, 1.2747, 1.9743, 2.5565, 3.0565, 3.5565, 4.0588, 4.5601, 5.2166, 5.9566) / (0.5081, 1.0551, 1.6007, 2.1007, 2.8604, 3.5328, 4.4931, 5.3080, 5.9194, 6.4195)	-18.62	22°
RUN	(0.5183, 1.2914, 1.9499, 2.5275, 3.0282, 3.5282, 4.0404, 4.5478, 5.2388, 5.9725) / (0.5050, 1.0099, 1.5207, 2.0236, 2.5240, 3.0351, 3.5432, 4.0480, 4.5540, 5.0773)	-18.59	22°
PSO	(0.7159, 1.5254, 2.1978, 2.7533, 3.2402, 3.7301, 4.2480, 4.7525, 5.4140, 6.1013) / (0.5067, 1.0718, 1.6279, 2.6383, 3.1684, 3.7125, 4.2425, 4.7523, 5.2525, 5.7528)	-18.59	22°

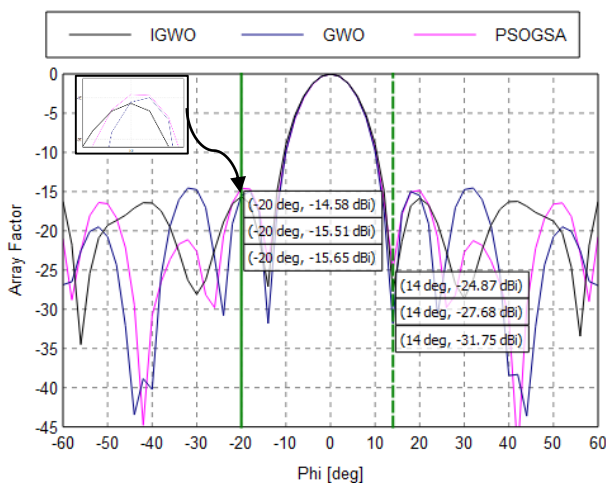


FIGURE 11. Normalized array factors of the 5 × 5 element PAA (position-only optimization) using EM FEKO software.

16.7 dB respectively. For GWO, GSA, RUN and PSO, SLL is -18.59 dB which is higher than I-GWO by 0.01 dB for same FNBW.

It can be concluded from examples 3 and 4, I-GWO results in more enhancements compared with other methods.

In the following, electromagnetic (EM) simulations using FEKO software are run to evaluate the effectiveness of various strategies in an EM environment, where it applied to example 3 for 5 × 5 PAA for element position optimization. Simulation results is shown in Fig. 11, where is compare the

radiation pattern using I-GWO, GWO and PSOGSA algorithms. It can be concluded that simulation using EM FEKO has result same results for SLL and FNBW in example 3, where it can be used effectively in real applications.

C. AMPLITUDE AND POSITION OPTIMIZATION

In this case, two-dimensional (2D) optimization is applied by controlling two array parameters: amplitude excitation and element position, while the phase excitation is fixed ($\beta_x = \beta_y = 0$). For SLL minimization, the array factor is written as:

$$AF_{PAA}(\theta, \varphi) = \sum_{m=1}^M e^{j(m-1)(kd_x \sin\theta \cos\varphi)} \sum_{n=1}^N e^{j(n-1)(kd_y \sin\theta \sin\varphi)} \quad (19)$$

Two cases were tested for a number of elements 5 × 5 and 10 × 10. For amplitude excitation optimization, the lower and upper limits X_L and X_U are set to 0 and 1, respectively. For element position optimization, the lower and upper limits X_L and X_U are set to 0.5 and 1, respectively. Simulation results are compared with other optimization algorithms; PSO, GSA, PSOGSA, GWO, SMA, and RUN. Example 5 illustrates the design optimization of 5 × 5 element antenna array. The sidelobe region is $\varphi_{SL} = [-80, -22]$. Fig. 12 shows the normalized array factors for the PAA. Table 6 compares the obtained results. SLL is -25.3 dB for I-GWO, while for GWO, and PSO, SLL is -25.11 dB and -25 dB which is higher than I-GWO by 0.19dB and 0.3dB for same FNBW. For GSA, RUN, PSOGSA and SMA, SLL is -24.73 dB, -19.3 dB, -18.42 dB and -17.39 dB respectively.

TABLE 6. FNBW and PSLL results for the 5 × 5 element PAA using 2D optimization (Amplitude excitations and elements positions optimization).

Method	Amplitude excitations $(A_{x1}, A_{x2}, \dots, A_{x5}) / (A_{y1}, A_{y2}, \dots, A_{y5})$ Element position $(d_{x1}, d_{x2}, \dots, d_{x5}) / (d_{y1}, d_{y2}, \dots, d_{y5})$	PSLL (dB)	FNBW
I-GWO	$(0.3946, 0.7887, 0.9739, 0.7593, 0.3580) / (0.8185, 0.0445, 0.5506, 0.9623, 0.1222)$ $(0.6923, 1.4384, 2.1850, 2.9271, 3.6692) / (0.6859, 1.2586, 1.9040, 2.4119, 3.2306)$	-25.3	44°
GWO	$(0.3440, 0.7681, 1.0000, 0.8222, 0.4305) / (0.0568, 0.00589, 0.3333, 0.1830, 0.3494)$ $(0.5135, 1.2595, 2.0052, 2.7495, 3.4915) / (0.8765, 1.7842, 2.4365, 3.2625, 4.1659)$	-25.11	44°
PSOGSA	$(0.5880, 0.9913, 0.9952, 0.4632, 0.5641) / (0.9998, 0.5912, 0.5753, 0.1487, 0.8585)$ $(0.5379, 1.2740, 1.8684, 2.5684, 3.1450) / (0.9210, 1.5210, 2.9508, 3.5619, 4.0542)$	-18.42	46°
GSA	$(0.2704, 0.6488, 0.8772, 0.7456, 0.4185) / (0.3352, 0.4893, 0.4142, 0.6118, 0.6448)$ $(0.6533, 1.3963, 2.1378, 2.8839, 3.6301) / (0.7197, 1.5622, 2.2006, 2.8471, 3.6822)$	-24.73	44°
RUN	$(0.3484, 0.7649, 1.0000, 0.8289, 0.4282) / (0.2969, 0.1354, 0.4571, 0.2547, 0.3850)$ $(0.5662, 1.2008, 1.7857, 2.3763, 3.0324) / (0.5817, 1.0961, 1.7063, 2.2996, 2.8780)$	-19.3	46°
SMA	$(0.6682, 0.7482, 0.9944, 1.0000, 0.7578) / (0.5000, 0.5000, 0.5000, 0.5943, 0.7462)$ $(0.7001, 1.4002, 2.1004, 2.8005, 3.5006) / (0.7001, 1.4002, 2.1004, 2.8005, 3.5006)$	-17.39	44°
PSO	$(0.2612, 0.5370, 0.7097, 0.5931, 0.2938) / (0.0057, 0.1362, 0.2520, 0.5286, 0.1453)$ $(0.6968, 1.4313, 2.1729, 2.9166, 3.6647) / (0.9912, 1.9334, 2.5388, 3.2228, 3.9250)$	-25	44°

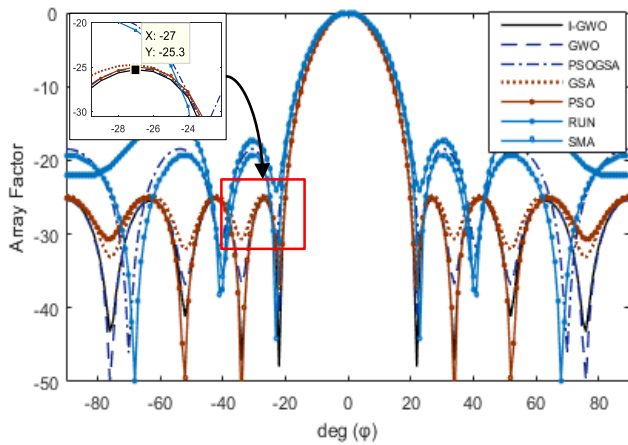


FIGURE 12. Normalized array factors of the 5 × 5 element PAA for amplitude and position optimization.

Example 6 illustrates the design optimization of 10 × 10 element antenna array. The sidelobe region is $\varphi_{SL} = [-80 -21]$. Fig. 13 shows the normalized array factors for the PAA. Table 7 compares the obtained results. SLL is -38.81 dB for I-GWO, while for GWO SLL is -32.57 dB which is higher than I-GWO by 6.24 dB for same FNBW. For SMA, PSO, GSA, PSOGSA and RUN SLL is -31.62 dB, -24 dB, -32.09 dB, -31.55 dB and -7.321 dB respectively. It also can be find that $A_y = 0$ for some elements in case of I-GWO and GWO, which mean lower power consumption in the overall array.

The application of 2D optimization using I-GWO for a 10 × 10 element antenna array results in SLL minimization with

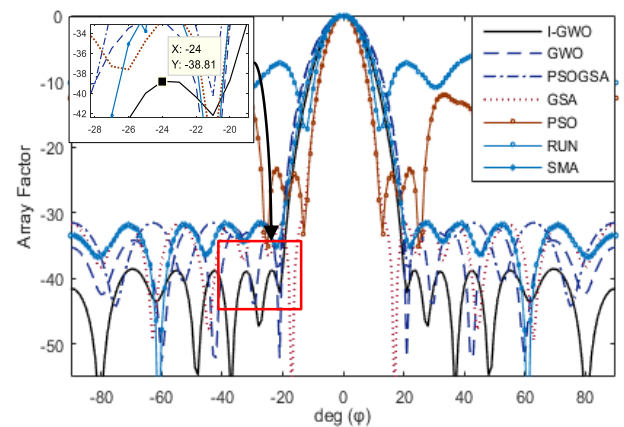


FIGURE 13. Normalized array factors of the 10 × 10 element PAA for amplitude and position optimization.

the minimized number of array elements, which results in a simple system design with reduced power and cost in comparing with single parameter optimization.

D. COMPUTATIONAL COMPLEXITY

In this section, computational time is computed for PAA beamforming optimization using I-GWO in the case of two parameter optimization (amplitude and position), and the results are compared with other algorithms; PSO, GSA, PSOGSA, GWO, SMA and RUN as shown in Table 8. The computational time measures the convergence time to obtain the optimum solution. I-GWO execution time is 6.043369 sec with a SLL of -38.81 dB. GWO execution time is 2.680383 sec for PSOGSA, GSA, RUN, SMA and PSO

TABLE 7. FNBW and PSLL results for the 10 × 10 elements PAA using 2D optimization (Amplitude excitations and elements positions optimization).

Method	Amplitude excitations ($A_{x1}, A_{x2}, \dots, A_{x10}$)/($A_{y1}, A_{y2}, \dots, A_{y10}$) Element position($d_{x1}, d_{x2}, \dots, d_{x10}$)/($d_{y1}, d_{y2}, \dots, d_{y10}$)	PSLL (dB)	FNBW
I-GWO	(0.0662, 0.0402, 0.1225, 0.3469, 0.7187, 0.9964, 0.8833, 0.8173, 0.6741, 0.2865)/ (0.0078, 0.0803, 0.7610, 0.0000, 0.6740, 0.0000, 0.4250, 0.0000, 0.0000, 0.5440) (0.6227, 1.1834, 1.8206, 2.6009, 3.3688, 4.0829, 4.6970, 5.2234, 5.8458, 6.5510) (0.6186, 1.1775, 1.7817, 2.3395, 3.0152, 3.7484, 4.6377, 5.4853, 6.0092, 6.9355)	-38.81	42°
GWO	(0.9003, 0.2179, 0.5401, 0.8049, 0.8064, 0.5253, 0.2030, 0.0002, 0.0007, 0.0000) / (0.8810, 0.9044, 0.0000, 0.0000, 0.0000, 1.0000, 0.0000, 1.0000, 0.0000, 0.4300) (0.9396, 1.7354, 2.4672, 3.2060, 3.9477, 4.6894, 5.4349, 6.3912, 7.3130, 8.1446) / (0.7392, 1.4458, 2.0199, 2.7473, 3.3113, 3.9679, 4.5953, 5.1739, 5.9421, 6.6671)	-32.57	42°
PSOGSA	(0.4619, 0.1004, 0.7552, 0.1140, 0.9966, 0.8099, 0.6795, 0.9216, 0.8769, 0.5465) / (0.9003, 0.1538, 0.3105, 0.1487, 0.8641, 0.1329, 0.1047, 0.1253, 0.4466, 0.1360) (0.9661, 1.6057, 1.7616, 1.8974, 2.5526, 3.4037, 4.3484, 5.2068, 6.0207, 6.7849) / (0.5016, 1.0633, 1.7655, 2.3705, 2.9234, 3.5178, 4.1817, 4.7608, 5.4915, 6.7819)	-31.55	42°
GSA	(0.3221, 0.5791, 0.6909, 0.5787, 0.4562, 0.5768, 0.8271, 0.8965, 0.6335, 0.2533) / (0.3609, 0.4653, 0.5075, 0.3633, 0.5765, 0.2570, 0.4813, 0.2664, 0.5012, 0.4558) (0.8925, 1.5820, 2.2914, 3.0102, 3.7636, 4.5424, 5.2845, 6.0127, 6.7408, 7.4817) / (0.7496, 1.6369, 2.4278, 3.2124, 3.8115, 4.5372, 5.2732, 5.8676, 6.5914, 7.4808)	-32.09	34°
SMA	(0.3743, 0.7211, 0.2163, 0.7574, 0.9210, 0.9206, 0.9967, 0.9229, 0.6552, 0.3284) / (0.1001, 0.1462, 0.1044, 0.1000, 0.1012, 0.1011, 0.1073, 0.1139, 0.1000, 0.1112) (0.5344, 1.4909, 2.8400, 3.6212, 4.2014, 4.6197, 5.4038, 5.9340, 6.6212, 7.5004) / (0.5714, 0.4685, 1.1191, 1.2359, 1.7645, 1.8645, 1.9645, 2.2449, 3.1497, 3.9709)	-31.62	44°
RUN	(0.7790, 0.4754, 0.7448, 1.0000, 0.6565, 0.5065, 0.4622, 0.4934, 0.7049, 0.9039) / (0.1001, 0.1000, 0.1000, 0.1004, 0.1000, 0.1274, 0.1498, 0.1854, 0.1221, 0.2219) (0.5262, 1.3007, 2.2298, 1.9296, 3.6630, 4.2851, 4.9268, 5.5284, 6.2151, 6.8312) / (0.5501, 1.2575, 1.7718, 2.5528, 3.7065, 4.5573, 5.3522, 6.0780, 6.7732, 7.5797)	-7.321	24°
PSO	(0.3221, 0.5791, 0.6909, 0.5787, 0.4562, 0.5768, 0.8271, 0.8965, 0.6335, 0.2533) / (0.3609, 0.4653, 0.5075, 0.3633, 0.5765, 0.2570, 0.4813, 0.2664, 0.5012, 0.4558) (0.8441, 1.8441, 2.8441, 3.6362, 4.6362, 5.6362, 6.5878, 7.0878, 8.0878, 8.6981) / (0.6573, 1.6237, 2.6237, 3.2726, 4.2726, 5.1389, 5.8861, 6.8861, 7.8006, 8.4773)	-24	26°

TABLE 8. Execution time for 2D optimization for 10 × 10 PAA.

Method	Time (sec)	PSLL (dB)
I-GWO	6.043369	-38.81
GWO	2.680383	-32.57
PSOGSA	3.316675	-31.55
GSA	2.084569	-32.09
RUN	4.054988	-7.321
SMA	3.425231	-31.62
PSO	1.537549	-24

execution time is 3.316675sec, 2.084569 sec, 4.054988 sec, 3.425231 sec and 1.537549 sec respectively. It can be concluded from the above analysis that I-GWO outperformed other techniques where it obtained the most suppressed SLL.

E. DISCUSSION OF RESULTS

In the previous examples, different analyses were performed to check the performance of PAA design and optimization

using the I-GWO algorithm by comparing it with other state-of-the-art algorithms. Table 9 compares all analysis results, for SLL in the three previous cases (amplitude only, position only, and 2D optimization), where the following results can be concluded:

In the case of amplitude only optimization, for 10 × 10 element array, SLL is minimized to -37.96 dB using I-GWO, which is minimized from PSOGSA by 0.48 dB, from GSA by 0.65 dB for the same FNBW and also lower than the other compared algorithms.

In the case of position only optimization, for 10 × 10 element array, SLL is minimized to -18.63 dB using I-GWO, which is minimized from SMA by 0.01dB, from GWO by 0.04 dB and from PSOGSA by 1.93 dB.

In comparing the previous two cases, I-GWO algorithms outperform other methods, especially when increasing the number of array elements.

In the case of 2D-optimization by optimizing both the amplitude and position of array elements, I-GWO results in the lowest SLL with the minimum number of elements. For 10 × 10 element array, I-GWO results -38.81 dB for 2D

TABLE 9. Comparison of PSLL (dB) in case of 10 × 10 elements PAA in case of amplitude only, position only, and 2D optimization.

Method	Amplitude only (10 × 10)	Position only (10 × 10)	2D (10 × 10)
I-GWO	-37.96	-18.63	-38.81
GWO	-36.99	-18.59	-32.57
PSOGSA	-37.48	-16.7	-31.55
GSA	-37.31	-18.59	-32.09
RUN	-36.82	-18.59	-7.321
SMA	-36.99	-18.62	-31.62
PSO	-37.13	-18.59	-24

TABLE 10. Comparison of PAA beamforming optimization using I-GWO with other previous works for different planar array geometries.

Method	No. of elements	PSLL (dB)	Directivity (dBi)
I-GWO	25	-25.3	18.77
	100	-38.81	20.45
BBO[27]	49	-20.96	17.14
	100	-20.82	20.27
TLBO[32]	84	-22.27	-
MFO [29]	30	-27.92	10.76
BSO [33]	100	-19.9	-
ICSO [28]	64	-14.09	-
WDO [34]	100	-25.83	19.72
GA [35]	100	-22.22	-

optimization, which is minimized from amplitude only by 0.85dB and from position only by 20.18 dB for the same number of elements.

In the previous analysis, it compared applying 2D optimization with single parameter optimization, which demonstrated the effectiveness of I-GWO in optimizing more than one array element.

In comparing the proposed 2D optimization using I-GWO with other algorithms, in the case of I-GWO, SLL is -38.81 dB which is minimized from GWO by 6.24 dB, from PSOGSA by 7.26 dB and from SMA by 7.19 dB.

From previous analysis, it can be concluded that the I-GWO method outperforms other techniques in applying 2D optimization, which provides SLL minimization with the saving of antenna array elements, which can lead to cost savings for the overall communication systems. In contrast, the other techniques obtained worse results using the 2D method compared with single element optimization.

The I-GWO approach is superior to other methods in the application of 2D optimization, which offers SLL reduction with the saving of antenna array components, which can

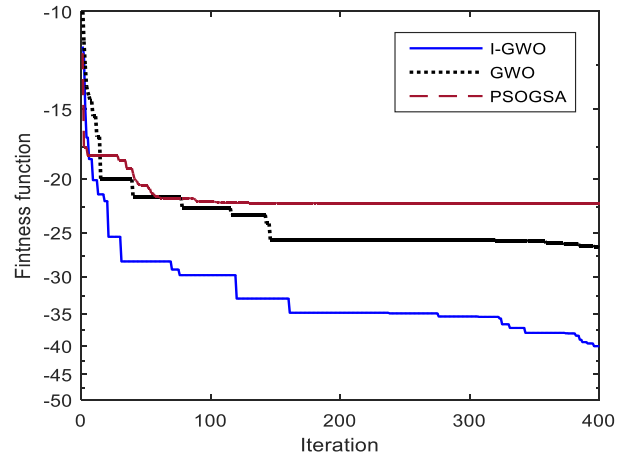


FIGURE 14. Convergence curve for I-GWO vs. GWO and PSOGSA.

result in cost savings for the entire communication system. This is based on past analysis. In contrast, when compared to single element optimization, the other strategies produced lower results when employing the 2D method.

Finally, in table 10 the comparison of PAA beamforming optimization using I-GWO with other previous work for different planar array geometries. That is clearly shows the effectiveness of I-GWO in PAA pattern synthesis for different number of array elements over the other works.

F. CONVERGENCE SPEED

This section compares I-GWO with PSOGSA and GWO in terms of convergence speed measured over 400 iterations. Fig. 14 shows that I-GWO converges to the solution faster than GWO and PSOGSA, which demonstrates the excellent performance of I-GWO as compared to other algorithms and how results can be enhanced for a larger number of iterations.

VI. CONCLUSION

This paper demonstrated the beamforming optimization effectiveness by using I-GWO algorithm for PAA in order to design more directive array for 5G applications. The optimization goal is to minimize the SLL for the PAA beam pattern. 2D optimization method is introduced and applied to PAA by optimizing both amplitude excitation and element positions. Simulation results show that the beamforming optimization of PAA using I-GWO provides enhancements when compared with results obtained using other techniques, especially in the case of 2D optimization, where it provides SLL minimization with a reduced number of antenna array elements. Also, the simulation results by EM FEKO software clearly shows that I-GWO is a very efficient algorithm that can be applied to solve different beamforming optimization problems and can be applied to real applications. It can also be applied to other antenna array geometries according to communication systems requirements.

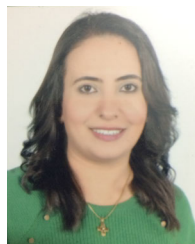
VII. FUTURE WORK

Antenna array beamforming using recent optimization algorithms is very helpful as it contributes to reducing system complexity and overall cost. Continuously, new optimization algorithms are presented. It is recommended in the future to use another recent optimization algorithm that can be introduced in the future to solve different beamforming optimization problems. Also, it is recommended to use different antenna array geometries that are required by different communication applications.

REFERENCES

- [1] M. A. Al-Absi, A. A. Al-Absi, M. Sain, and H. J. Lee, "A state of the art: Future possibility of 5G with IoT and other challenges," in *Smart Healthcare Analytics in IoT Enabled Environment*, vol. 178, P. Patnaik, and S. Mohanty, Eds. Cham, Switzerland: Springer, 2020, pp. 35–65.
- [2] S. Ghosh and D. Sen, "An inclusive survey on array antenna design for millimeter-wave communications," *IEEE Access*, vol. 7, pp. 83137–83161, 2019.
- [3] V. Dakulagi and M. Bakhar, "Advances in smart antenna systems for wireless communication," *Wireless Pers. Commun.*, vol. 110, no. 2, pp. 931–957, Jan. 2020.
- [4] S. K. Goudos, P. D. Diamantoulakis, and G. K. Karagiannidis, "Multi-objective optimization in 5G wireless networks with massive MIMO," *IEEE Commun. Lett.*, vol. 22, no. 11, pp. 2346–2349, Nov. 2018.
- [5] A. Chakraborty, G. Ram, and D. Mandal, "Optimal pulse shifting in timed antenna array for simultaneous reduction of sidelobe and sideband level," *IEEE Access*, vol. 8, pp. 131063–131075, 2020.
- [6] S. Poddar, P. Paul, A. Chakraborty, G. Ram, and D. Mandal, "Design optimization of linear arrays and time-modulated antenna arrays using meta-heuristics approach," *Int. J. Numer. Modelling, Electron. Netw., Devices Fields*, vol. 35, no. 5, Sep. 2022, Art. no. e3010.
- [7] A. Chakraborty, G. Ram, and D. Mandal, "Time-modulated linear array synthesis with optimal time schemes for the simultaneous suppression of sidelobe and sidebands," *Int. J. Microw. Wireless Technol.*, vol. 14, no. 6, pp. 768–780, Jul. 2022.
- [8] B. Goswami and D. Mandal, "A genetic algorithm for the level control of nulls and sidelobes in linear antenna arrays," *J. King Saud Univ. Comput. Inf. Sci.*, vol. 25, no. 2, pp. 117–126, 2013.
- [9] F. Enache, D. Deperateanu, and F. Popescu, "Optimal design of circular antenna array using genetic algorithms," in *Proc. 9th Int. Conf. Electron., Comput. Artif. Intell. (ECAI)*, Jun. 2017, pp. 1–6.
- [10] M. Khodier, "Comprehensive study of linear antenna array optimisation using the cuckoo search algorithm," *IET Microw., Antennas Propag.*, vol. 13, no. 9, pp. 1325–1333, Jul. 2019.
- [11] U. Singh and M. Rattan, "Design of linear and circular antenna arrays using cuckoo optimization algorithm," *Prog. Electromagn. Res. C*, vol. 46, pp. 1–11, 2014.
- [12] M. M. Khodier and M. Al-Aqeel, "Linear and circular array optimization: A study using particle swarm intelligence," *Prog. Electromagn. Res. B*, vol. 15, pp. 347–373, 2009.
- [13] L. A. Greda, A. Winterstein, D. L. Lemes, and M. V. T. Heckler, "Beamsteering and beamshaping using a linear antenna array based on particle swarm optimization," *IEEE Access*, vol. 7, pp. 141562–141573, 2019.
- [14] S. U. Rahman, Q. Cao, M. M. Ahmed, and H. Khalil, "Analysis of linear antenna array for minimum side lobe level, half power beamwidth, and nulls control using PSO," *J. Microw., Optoelectron. Electromagn. Appl.*, vol. 16, no. 2, pp. 577–591, Apr. 2017.
- [15] P. Swain, S. K. Mohanty, and B. B. Mangaraj, "Linear dipole antenna array design and optimization using gravitational search algorithm," in *Proc. 2nd Int. Conf. Adv. Electr., Electron., Inf., Commun. Bio-Inform. (AEEICB)*, Feb. 2016, pp. 514–518.
- [16] A. Sharma, S. Mathur, and R. Gowri, "Adaptive beamforming for linear antenna arrays using gravitational search algorithm," in *Proc. Intell. Commun., Control Devices (ICICCD)*. Singapore: Springer, 2017, pp. 1159–1169.
- [17] L. Liu, A. Wang, G. Sun, T. Zheng, and C. Yu, "An improved biogeography-based optimization approach for beam pattern optimizations of linear and circular antenna arrays," *Int. J. Numer. Modelling, Electron. Netw., Devices Fields*, vol. 34, no. 6, Nov. 2021, Art. no. e2910.
- [18] E. O. Owoola, K. Xia, T. Wang, A. Umar, and R. G. Akindele, "Pattern synthesis of uniform and sparse linear antenna array using mayfly algorithm," *IEEE Access*, vol. 9, pp. 77954–77975, 2021.
- [19] H. Wang, C. Liu, H. Wu, B. Li, and X. Xie, "Optimal pattern synthesis of linear array and broadband design of whip antenna using grasshopper optimization algorithm," *Int. J. Antennas Propag.*, vol. 2020, pp. 1–14, Jan. 2020.
- [20] Q. Liang, B. Chen, H. Wu, C. Ma, and S. Li, "A novel modified sparrow search algorithm with application in side lobe level reduction of linear antenna array," *Wireless Commun. Mobile Comput.*, vol. 2021, pp. 1–25, Jun. 2021.
- [21] A. I. Mohsin, A. S. Daghfal, and A. H. Sallomi, "A beamforming study of the linear antenna array using grey wolf optimization algorithm," *Indonesian J. Electr. Eng. Comput. Sci.*, vol. 20, pp. 1538–1546, Dec. 2020.
- [22] P. Saxena and A. Kothari, "Optimal pattern synthesis of linear antenna array using grey wolf optimization algorithm," *Int. J. Antennas Propag.*, vol. 2016, pp. 1–11, Apr. 2016.
- [23] A. Recioui, "Optimization of Circular antenna arrays using a differential search algorithm," *Acta Phys. Polonica A*, vol. 128, pp. 7–8, Aug. 2015.
- [24] H. Ullah and F. A. Tahir, "Broadband planar antenna array for future 5G communication standards," *IET Microw., Antennas Propag.*, vol. 13, no. 15, pp. 2661–2668, Dec. 2019.
- [25] T. Prabhu and S. C. Pandian, "Design and development of planar antenna array for MIMO application," *Wireless Netw.*, vol. 27, no. 2, pp. 939–946, Feb. 2021.
- [26] K. N. A. Rani, M. Abdulmalek, H. A. Rahim, N. S. Chin, and A. A. Wahab, "Hybridization of strength Pareto multiobjective optimization with modified cuckoo search algorithm for rectangular array," *Sci. Rep.*, vol. 7, no. 1, Apr. 2017, Art. no. 46521.
- [27] A. Recioui, N. Arhab, and I. Zeghad, "Pattern design of 2D antenna arrays using biogeography based optimization," *Int. J. Comput. Sci., Commun. Inf. Technol. (CSCIT)*, vol. 2019, vol. 6, no. 2, pp. 38–43.
- [28] S. Liang, Z. Fang, G. Sun, Y. Liu, G. Qu, and Y. Zhang, "Sidelobe reductions of antenna arrays via an improved chicken swarm optimization approach," *IEEE Access*, vol. 8, pp. 37664–37683, 2020.
- [29] A. Das, D. Mandal, S. P. Ghoshal, and R. Kar, "Concentric circular antenna array synthesis for side lobe suppression using moth flame optimization," *AEU Int. J. Electron. Commun.*, vol. 86, pp. 177–184, Mar. 2018.
- [30] G. Oliveri, L. Poli, and A. Massa, "Maximum efficiency beam synthesis of radiating planar arrays for wireless power transmission," *IEEE Trans. Antennas Propag.*, vol. 61, no. 5, pp. 2490–2499, May 2013.
- [31] G. Shen, Y. Liu, G. Sun, T. Zheng, X. Zhou, and A. Wang, "Suppressing sidelobe level of the planar antenna array in wireless power transmission," *IEEE Access*, vol. 7, pp. 6958–6970, 2019.
- [32] K. P. Dutta, G. K. Mahanti, and G. Panda, "Effective minimization of side lobe level of sparse thinned planar array antenna in multiple planes with constraints," *Electromagnetics*, vol. 41, no. 5, pp. 303–314, Jul. 2021.
- [33] J. Chen, N. Bulgan, X. Xue, X. Fan, and X. Zhang, "Planar thinned antenna array synthesis using modified brain storm optimization," in *Proc. Int. Conf. Swarm Intell.* Chiang Mai, Thailand: Springer, Jul. 2019, pp. 276–285.
- [34] A. Recioui, M. Benabid, and N. Djilani, "Rectangular antenna array optimization using wind driven optimization," *Algerian J. Signals Syst.*, vol. 1, no. 2, pp. 109–120, Feb. 2021.
- [35] A. Reyna and M. A. Panduro, "Optimization of a scannable pattern for uniform planar antenna arrays to minimize the side lobe level," *J. Electromagn. Waves Appl.*, vol. 22, no. 16, pp. 2241–2250, Jan. 2008.
- [36] K.-J. Oh, H.-Y. Lee, S.-J. Kim, Y.-S. Chung, and C. Cheon, "A study on wideband adaptive beamforming using Taylor weighting and LSMI algorithm," *Trans. Korean Inst. Electr. Eng.*, vol. 62, no. 3, pp. 380–386, Mar. 2013.
- [37] Y. P. Saputra, F. Oktafiani, Y. Wahyu, and A. Munir, "Side lobe suppression for X-band array antenna using Dolph–Chebyshev power distribution," in *Proc. 22nd Asia-Pacific Conf. Commun. (APCC)*, Aug. 2016, pp. 86–89.
- [38] X. Zhao, Q. Yang, and Y. Zhang, "Design of non-uniform circular antenna arrays by convex optimization," in *Proc. 10th Eur. Conf. Antennas Propag. (EuCAP)*, Apr. 2016, pp. 1–4.
- [39] S. K. Goudos, C. Kalialakis, and R. Mitra, "Evolutionary algorithms applied to antennas and propagation: A review of state of the art," *Int. J. Antennas Propag.*, vol. 2016, pp. 1–12, Jan. 2016.
- [40] A. A. Heidari, S. Mirjalili, H. Farris, I. Aljarah, M. Mafarja, and H. Chen, "Harris hawks' optimization: Algorithm and applications," *Future Gener. Comput. Syst.*, vol. 97, pp. 849–872, Aug. 2019.

- [41] H. M. Alabool, D. Alarabiat, L. Abualigah, and A. A. Heidari, "Harris hawks optimization: A comprehensive review of recent variants and applications," *Neural Comput. Appl.*, vol. 33, no. 15, pp. 8939–8980, Aug. 2021.
- [42] V. K. Kamboj, A. Nandi, A. Bhadoria, and S. Sehgal, "An intensify Harris hawks optimizer for numerical and engineering optimization problems," *Appl. Soft Comput.*, vol. 89, Apr. 2020, Art. no. 106018.
- [43] S. Li, H. Chen, M. Wang, A. A. Heidari, and S. Mirjalili, "Slime mould algorithm: A new method for stochastic optimization," *Future Gener. Comput. Syst.*, vol. 111, pp. 300–323, Oct. 2020.
- [44] H. Chen, C. Li, M. Mafarja, A. A. Heidari, Y. Chen, and Z. Cai, "Slime mould algorithm: A comprehensive review of recent variants and applications," *Int. J. Syst. Sci.*, vol. 54, no. 1, pp. 204–235, Jan. 2023.
- [45] A. R. Jordehi, "Binary particle swarm optimisation with quadratic transfer function: A new binary optimisation algorithm for optimal scheduling of appliances in smart homes," *Appl. Soft Comput.*, vol. 78, pp. 465–480, May 2019.
- [46] A. Magdy, K. R. Mahmoud, and S. Sayed, "Cooperative communications based smart antenna systems using PSO algorithm," in *Proc. PIERS*, vol. 15, Stockholm, Sweden, Aug. 2013, pp. 600–615.
- [47] A. R. Jordehi, "Enhanced leader particle swarm optimisation (ELPSO): An efficient algorithm for parameter estimation of photovoltaic (PV) cells and modules," *Sol. Energy*, vol. 159, pp. 78–87, Jan. 2018.
- [48] A. R. Jordehi, "A mixed binary-continuous particle swarm optimisation algorithm for unit commitment in microgrids considering uncertainties and emissions," *Int. Trans. Electr. Energy Syst.*, vol. 30, no. 11, Nov. 2020, Art. no. e12581.
- [49] I. Ahmadianfar, A. A. Heidari, A. H. Gandomi, X. Chu, and H. Chen, "RUN beyond the metaphor: An efficient optimization algorithm based on Runge Kutta method," *Expert Syst. Appl.*, vol. 181, Nov. 2021, Art. no. 115079.
- [50] B. S. Yıldız, P. Mehta, N. Panagant, S. Mirjalili, and A. R. Yıldız, "A novel chaotic Runge Kutta optimization algorithm for solving constrained engineering problems," *J. Comput. Design Eng.*, vol. 9, no. 6, pp. 2452–2465, Dec. 2022.
- [51] S. Mirjalili and S. Z. M. Hashim, "A new hybrid PSO-GSA algorithm for function optimization," in *Proc. Int. Conf. Comput. Inf. Appl.*, Dec. 2010, pp. 374–377.
- [52] A. Magdy, O. M. EL-Ghandour, and H. F. A. Hamed, "Performance enhancement for adaptive beam-forming application based hybrid PSO-GSA algorithm," *J. Electromagn. Anal. Appl.*, vol. 7, no. 4, pp. 126–133, 2015.
- [53] S. Mirjalili, S. M. Mirjalili, and A. Lewis, "Grey wolf optimizer," *Adv. Eng. Softw.*, vol. 69, pp. 46–61, Mar. 2014.
- [54] H. Faris, I. Aljarah, M. A. Al-Betar, and S. Mirjalili, "Grey wolf optimizer: A review of recent variants and applications," *Neural Comput. Appl.*, vol. 30, no. 2, pp. 413–435, Jul. 2018.
- [55] M. R. S. Malik, E. R. Mohideen, and L. Ali, "Weighted distance grey wolf optimizer for global optimization problems," in *Proc. IEEE Int. Conf. Comput. Intell. Comput. Res. (ICCCIC)*, Dec. 2015, pp. 1–6.
- [56] T. Jayabarathi, T. Raghunathan, B. R. Adarsh, and P. N. Suganthan, "Economic dispatch using hybrid grey wolf optimizer," *Energy*, vol. 111, pp. 630–641, Sep. 2016.
- [57] N. Singh and S. B. Singh, "A novel hybrid GWO-SCA approach for optimization problems," *Eng. Sci. Technol., Int. J.*, vol. 20, no. 6, pp. 1586–1601, Dec. 2017.
- [58] A. A. Alomoush, A. A. Alsewari, H. S. Alamri, K. Aloufi, and K. Z. Zamli, "Hybrid harmony search algorithm with grey wolf optimizer and modified opposition-based learning," *IEEE Access*, vol. 7, pp. 68764–68785, 2019.
- [59] M. H. Nadimi-Shahraki, S. Taghian, and S. Mirjalili, "An improved grey wolf optimizer for solving engineering problems," *Expert Syst. Appl.*, vol. 166, Mar. 2021, Art. no. 113917.
- [60] X. Liu, Y. Wang, and M. Zhou, "Dimensional learning strategy-based grey wolf optimizer for solving the global optimization problem," *Comput. Intell. Neurosci.*, vol. 2022, pp. 1–31, Jan. 2022.
- [61] C. A. Balanis, *Antenna Theory: Analysis and Design*, 4th ed. Hoboken, NJ, USA: Wiley, 2016.
- [62] D. H. Wolpert and W. G. Macready, "No free lunch theorems for optimization," *IEEE Trans. Evol. Comput.*, vol. 1, no. 1, pp. 67–82, Apr. 1997.



NANCY GHATTAS received the B.S. degree in electronics and communications engineering and the M.Sc. degree in communication engineering from Suez Canal University, Egypt, in 2007 and 2018, respectively, where she is currently pursuing the Ph.D. degree in communication engineering. Her research interests include smart antennas, beamforming, and wireless communications.



ATEF M. GHUNIEM received the B.Sc. and M.Sc. degrees in electrical engineering from the Military Technical College (MTC), Cairo, Egypt, in 1971 and 1979, respectively, and the Ph.D. degree in electrical engineering (major areas: electrophysics, electronics, and waves) from The George Washington University, Washington, DC, USA, in 1985. He was a Staff Member with the Electrical Engineering Department, MTC, from 1975 to 1996. From 1998 to 2008, he was an Associate Professor with the Electrical Engineering Department, Faculty of Engineering, Suez Canal University, where he has been a Professor Emeritus, since 2008. His research interests include antennas and electromagnetic wave propagation, metamaterials, passive and active microwave devices, wireless communication, cognitive radio, and wireless sensor networks.



ABDELAZEEM A. ABDELSALAM (Member, IEEE) received the B.Sc., M.Sc., and Ph.D. degrees in electrical engineering from Suez Canal University, Egypt, in 2001, 2005, and 2011, respectively. He is currently an Associate Professor with Suez Canal University. He was a Postdoctoral Fellow with the Institute of Technology (UOIT), University of Ontario, Canada. He has authored or coauthored more than 60 refereed journals and conference papers and three book chapters. His research interests include power quality, D-FACTS technology, switched filter compensators, micro-grid interface, and control and application of artificial intelligence techniques in power systems.



AHMED MAGDY (Member, IEEE) was born in Cairo, Egypt, in 1986. He received the B.S. degree in electronic and communication engineering and the M.Sc. degree in communication engineering from Helwan University, Egypt, in 2008 and 2013, respectively, and the Ph.D. degree in electrical engineering, communication branch from Minia University, Egypt, in 2017. He is currently an Assistant Professor in communication branch with the Electrical Engineering Department, Suez Canal University, Ismailia, Egypt. His research interests include embedded systems, MEMS, image/signal processing AI, the IoT, computer vision, and smart antenna. He is a reviewer of the IET journals.